Inorganic Chemistry
Article

Inorg. Chem. **2010**, *49*, 2111–2122 **2111**
DOI: 10.1021/ic9015993

Reactions of a Phosphinoaldehyde with Pd^{II}, Rh^{I}, and Ir^{I} Precursors, Including the Formation of Complexes Containing a P,OH-Chelated Phosphinohemiacetal Ligand: a New Bonding Mode

Fabio Lorenzini, Dmitry Moiseev, Brian O. Patrick, and Brian R. James*

Department of Chemistry, University of British Columbia, Vancouver, British Columbia, Canada V6T 1Z1

Received August 11, 2009

The complexes *trans*-$PdCl_2[\eta^1$-*P*-$(Ph_2P)CH(Ph)CH(Me)CH(OMe)_2]_2$ (**1**) and $M(H)Cl[\eta^2$-*P*,*O*H-$(Ph_2P)CH(Ph)$-$CH(Me)CH(OH)OMe][\eta^2$-*P*,*C*(O)-$(Ph_2P)CH(Ph)CH(Me)C(O)]$, M = Rh (**3**) and Ir (**4**), are synthesized by reacting the phosphinoaldehyde [3-(diphenylphosphino)-3-phenyl-2-methyl]propionaldehyde $[(Ph_2P)_2CH(Ph)CH(Me)CHO]$ with *trans*-$PdCl_2(PhCN)_2$, $[RhCl(COD)]_2$, and $[IrCl(COD)]_2$, respectively, in MeOH; *trans*-$PdCl_2[\eta^1$-*P*-$(Ph_2P)CH(Ph)$-$CH(Me)CHO]_2$ (**2**) is isolated from the same reaction in CH_2Cl_2. One diastereomer of each of the complexes **1**, **3**·MeOH, and **4**·MeOH was characterized by X-ray analysis. The stereochemistry of such complexes in the solid state and in solution (MeOH and CH_2Cl_2) is discussed. In CD_2Cl_2, NMR data suggest that the coordinated hemiacetal moiety of **3** (but not **4**) undergoes reversible loss of MeOH; this process is associated with equilibria between various diastereomers of **3** that were investigated by $^{31}P\{^1H\}$, $^{13}C\{^1H\}$, ^1H, $^1H\{^{31}P\}$, and HSQC and HMBC $^1H/^{31}P\{^1H\}$ and $^1H/^{13}C\{^1H\}$ NMR spectroscopies. Complexes **3** and **4** reveal a new chelate bonding mode via a P atom and the hydroxyl O atom of a hemiacetal. Solvent-dependent stereochemical changes within solution species imply that such chiral phosphinoaldehydes are not likely to be useful ligands for applications in asymmetric catalysis, although conditions are suggested for testing the complexes as potential precursors for nonasymmetric catalytic processes.

Introduction

Our group reported recently on the isolation of new tertiary phosphines of the type $(Ph_2P)CH(Ar)CH_2CHO$ (Ar = Ph, *p*-tol, and *p*-$OMeC_6H_4$) from the 1:1 hydrophosphination of the olefinic bond of cinnamaldehydes (and substituted ones) with Ph_2PH;[1] (*Z*)-α-methylcinnamaldehyde similarly afforded $(Ph_2P)CH^*(Ph)C^*H(Me)CHO$ (abbreviated **P-CHO**), which was isolated as a mixture of diastereomers with predominantly *S*,*S* and *R*,*R* configurations at the C atoms (C*) but with a high diastereomeric ratio (dr) of ∼20;[1] subsequent hydrophosphination of the −CHO group generated an α-hydroxybis(phosphine) with a further chiral C center.[1] We have now initiated studies on the coordination chemistry of **P-CHO** with platinum metals often associated with homogeneous catalysis (Pd, Rh, and Ir) with the aim of investigating how such phosphinoaldehyde ligands interact with these metals, with a view of the potential of such metal−ligand systems for catalysis. This phosphinoaldehyde was chosen for study because it was found to readily generate crystalline products upon reaction with platinum metal precursors.

Much attention has been paid to the use of phosphinoaldehyde ligands that contain the "soft" P atom and "harder" aldehyde O atom, and reported binding modes are outlined in Scheme 1 (envisioned for the aldehyde that we studied): (a) simple, monodentate η^1-P coordination;[2] (b) subsequent oxidative addition of the aldehyde C−H bond at the metal center, which is one procedure for the generation of *cis*-hydridophosphinoacyl/aroyl complexes (H, η^2-PC mode);[3] (c) a chelating mode formed with a σ-bonded aldehyde O atom (η^2-PO mode);[3r,4] (d) a rarer chelating mode involving a π-bonded carbonyl (η^3-PCO mode).[5]

In this paper, we report the reactions of **P-CHO** with Pd^{II}, Rh^{I}, and Ir^{I} precursors in MeOH and in CH_2Cl_2. Findings establish the η^1-P binding mode, the acyl hydrido η^2-PC mode, and either the η^2-PO or η^3-PCO mode of the phosphinoaldehyde. Studies on the Pd^{II} system in MeOH reveal also the η^1-P binding mode for the acetal derivative of the phosphinoaldehyde. Studies carried out on the Rh and Ir systems in MeOH, where the carbonyl moiety can exist as a hemiacetal, reveal also a novel chelated phosphinohemiacetal in which the hemiacetal binds in a σ fashion through the

*To whom correspondence should be addressed. E-mail: brj@chem.ubc.ca.

(1) Moiseev, D. V.; Patrick, B. O.; James, B. R. *Inorg. Chem.* **2007**, *46*, 11467.

(2) For example, see:(a) El Mail, R.; Garralda, M. A.; Hernández, R.; Ibarlucea, L. *J. Organomet. Chem.* **2002**, *648*, 149. (b) Ainscough, E. W.; Brodie, A. M.; Ingham, S. L.; Waters, J. M. *Inorg. Chim. Acta* **1995**, *234*, 163. (c) Schumann, H.; Hemling, H.; Ravindar, V.; Badrieh, Y.; Blum, J. *J. Organomet. Chem.* **1994**, *469*, 213.

Published on Web 02/05/2010

Scheme 1. Possible Binding Modes of $(Ph_2P)CH(Ph)CH(Me)CHO$, Abbreviated **P-CHO**

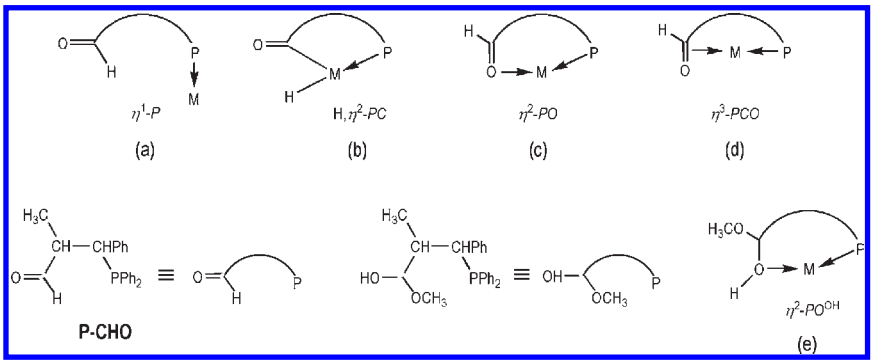

hydroxyl O atom (η^2-PO^{OH} mode; Scheme 1e). Aspects of the stereochemistry at the C atoms in the various complexes (both in the solid state and in solution, where diastereomeric changes are noted) are also considered and lead us to comment on the potential application of the species in asymmetric catalysis. Our findings on the solution behavior are relevant for others considering the use of chiral phosphinoaldehyde-liganded systems for such catalysis.

Use of the nonchiral $Ph_2PCH_2CH_2CHO$ ligand would necessarily lead to simpler metal complex systems, but as noted in a publication[6] that appeared after our paper was submitted, this phosphinoaldehyde is not formed by the addition of Ph_2PH to acrolein; however, this reaction in the presence of a Pd^{II} complex does generate a complex containing η^1-*P*-$Ph_2PCH_2CH_2CHO$. The subsequent addition of Ph_2PH across the free CHO group of the coordinated phosphinoaldehyde generated coordinated $Ph_2P(CH_2)_2C^*H(PPh_2)OH$ with a chiral C*, and the use of an auxiliary chiral amine at the Pd allowed for isolation of the enantiomerically pure functionalized diphosphine.[6]

Experimental Section

General Procedures. *trans*-$PdCl_2(PhCN)_2$,[7] $[RhCl(COD)]_2$,[8] and $[IrCl(COD)]_2$[9] were synthesized by literature procedures from chloride precursors (purchased from Colonial Metals Inc.). The phosphinoaldehyde **P-CHO**, available as a mixture of diastereomers (dr ~ 20), was synthesized by our reported method,[1] and its reactions with the Pd, Rh, and Ir complexes were carried out under Ar using Schlenk techniques or in a J. Young NMR tube; MeOH, CH_2Cl_2, and Et_2O were dried over Mg/I_2, CaH_2, and sodium benzophenone ketyl, respectively, and distilled under N_2. $^{31}P\{^1H\}$, $^{13}C\{^1H\}$, ^1H, and $^1H\{^{31}P\}$ NMR spectra were measured in CD_3OD or CD_2Cl_2, as indicated, at room temperature (rt ~300 K) on a Bruker AV400 spectrometer. All shifts are reported in ppm (s = singlet, d = doublet, t = triplet, q = quintet, m = multiplet, and br = broad), relative to external $SiMe_4$ or 85% aqueous H_3PO_4, with *J* values given in Hertz. When necessary, atom assignments were made by means of HSQC and HMBC $^1H/^{31}P\{^1H\}$ and $^1H/^{13}C\{^1H\}$ NMR correlation spectroscopies. Residual protonated species in the deuterated solvents were used as internal references (δ 5.32 t for CD_2Cl_2; δ 3.31 q and 4.87 s for CD_3OD). Solid samples of the synthesized complexes were stored at rt under Ar. Elemental analyses were performed on a Carlo Erba 1108 analyzer. MALDI-MS were obtained on a Bruker Biflex IV MALDI-TOF spectrometer equipped with a N laser; the samples were dissolved in acetone/MeOH or CH_2Cl_2/MeOH, and dithranol was used as the matrix. The sample solutions (~1 mg mL^{-1}) and the matrix (~20 mg mL^{-1}) were mixed in a ratio of 1:1 to 1:10, and 1 μL of the mixture was deposited onto the sample target; these spectra were acquired in the positive reflection mode with delay extraction by averaging 100 laser shots and were calibrated externally using peptides. MS data are reported as *m*/*z* values. IR spectra (cm^{-1}) were measured with a Thermo Nicolet FT-IR Nexus spectrometer using samples in either Nujol or CH_2Cl_2.

***trans*-$PdCl_2[\eta^1$-*P*-$(Ph_2P)CH(Ph)CH(Me)CH(OMe)_2]_2$ (1).** **P-CHO** (87.0 mg, 0.262 mmol) was added to a MeOH solution (~5 mL) of *trans*-$PdCl_2(PhCN)_2$ (50.0 mg, 0.131 mmol) under Ar, and the reaction mixture was stirred for 18 h at rt. Deposited yellow crystals of **1** were filtered off, washed with MeOH (~1 mL), and dried overnight under vacuum (80.0 mg, 66% yield). Anal. Calcd for $C_{48}H_{54}Cl_2O_4P_2Pd$: C, 61.71; H, 5.83. Found: C, 61.70; H, 5.79. Complex **1** precipitates as diastereomer **1a** (a mixture of *S*,*S*/*R*,*R* and *R*,*R*/*S*,*S* enantiomers), with small impurities due to the minor diastereomer of the starting phosphine (see the text); **1a** dissolves in CD_2Cl_2 and over 2 days forms diastereomer **1b** [a mixture of *S*,*S*/*S*,*S* and *R*,*R*/*R*,*R* enantiomers (see the text)].

(3) For example, see:(a) Cao, C.; Wang, T.; Patrick, B. O.; Love, J. A. *Organometallics* **2006**, *25*, 1321. (b) Garralda, M. A.; Hernández, R.; Ibarlucea, L.; Pinilla, E.; Torres, M. R.; Zarandona, M. *Inorg. Chim. Acta* **2004**, *357*, 2818. (c) Garralda, M. A.; Hernández, R.; Ibarlucea, L.; Pinilla, E.; Torres, M. R. *Organometallics* **2003**, *22*, 3600. (d) Cîrcu, V.; Fernandes, M. A.; Carlton, L. *Inorg. Chem.* **2002**, *41*, 3859. (e) Goikhman, R.; Milstein, D. *Angew. Chem., Int. Ed.* **2001**, *40*, 1119. (f) El Mail, R.; Garralda, M. A.; Hernández, R.; Ibarlucea, L.; Pinilla, E.; Torres, M. R. *Organometallics* **2000**, *19*, 5310. (g) Peterson, T. H.; Golden, J. T.; Bergman, R. G. *Organometallics* **1999**, *18*, 2005. (h) Klein, H.-F.; Lemke, U.; Lemke, M.; Brand, A. *Organometallics* **1998**, *17*, 4196. (i) Wang, K.; Emge, T. J.; Goldman, A. S.; Li, C.; Nolan, S. P. *Organometallics* **1995**, *14*, 4929. (j) Bleeke, J. R.; Haile, T.; New, P. R.; Chiang, M. Y. *Organometallics* **1993**, *12*, 517. (k) Bianchini, C.; Meli, A.; Peruzzini, M.; Vizza, F.; Bachechi, F. *Organometallics* **1991**, *10*, 820. (l) Bianchini, C.; Meli, A.; Peruzzini, M.; Ramirez, J. A.; Vacca, A.; Vizza, F.; Zanobini, F. *Organometallics* **1989**, *8*, 337. (m) Ghilardi, C. A.; Midollini, S.; Moneti, S.; Orlandini, A. *J. Chem. Soc., Dalton Trans.* **1988**, 1833. (n) Milstein, D.; Fultz, W. C.; Calabrese, J. C. *J. Am. Chem. Soc.* **1986**, *108*, 1336. (o) Koh, J. J.; Lee, W.-H.; Williard, P. G.; Risen, W. M., Jr. *J. Organomet. Chem.* **1985**, *284*, 409. (p) Dahlenburg, L.; Mirzaei, F. *J. Organomet. Chem.* **1983**, *251*, 103. (q) Landvatter, E. F.; Rauchfuss, T. B. *Organometallics* **1982**, *1*, 506. (r) Rauchfuss, T. B. *J. Am. Chem. Soc.* **1979**, *101*, 1045.

(4) For example, see:(a) El Mail, R.; Garralda, M. A.; Hernández, R.; Ibarlucea, L.; Pinilla, E.; Torres, M. R. *Helv. Chim. Acta* **2002**, *85*, 1485. (b) Chen, X.; Femia, F. J.; Babich, J. W.; Zubieta, J. *Inorg. Chim. Acta* **2001**, *315*, 147.

(5) For example, see:(a) Yeh, W.-Y.; Lin, C.-S.; Peng, S.-M.; Lee, G.-H. *Organometallics* **2004**, *23*, 917. (b) Lenges, C. P.; Brookhart, M.; White, P. S. *Angew. Chem., Int. Ed.* **1999**, *38*, 552. (c) Blaschke, U.; Menges, F.; Erker, G.; Fröhlich, R. *Eur. J. Inorg. Chem.* **1999**, 621. (d) Adams, H.; Bailey, N. A.; Gauntlett, J. T.; Winter, M. J. *J. Chem. Soc., Chem. Commun.* **1984**, 1360.

(6) Yuan, M.; Zhang, N.; Pullarkat, S. A.; Li, Y.; Liu, F.; Pham, P.-T.; Leung, P.-H. *Inorg. Chem.* **2010**, *49*, DOI 10.1021/ic9018053.

(7) (a) Hartley, F. R. *Organomet. Rev. A* **1976**, *6*, 119. (b) Kharasch, M. S.; Seyler, R. C.; Mayo, F. R. *J. Am. Chem. Soc.* **1938**, *60*, 882.

(8) Schenck, T. G.; Downes, J. M.; Milne, C. R. C.; MacKenzie, P. B.; Boucher, H.; Whelan, J.; Bosnich, B. *Inorg. Chem.* **1985**, *24*, 2334.

(9) Herde, J. L.; Lambert, J. C.; Senoff, C. V. *Inorg. Synth.* **1974**, *15*, 18.

Scheme 2. Synthesis of **1** and **2**[a]

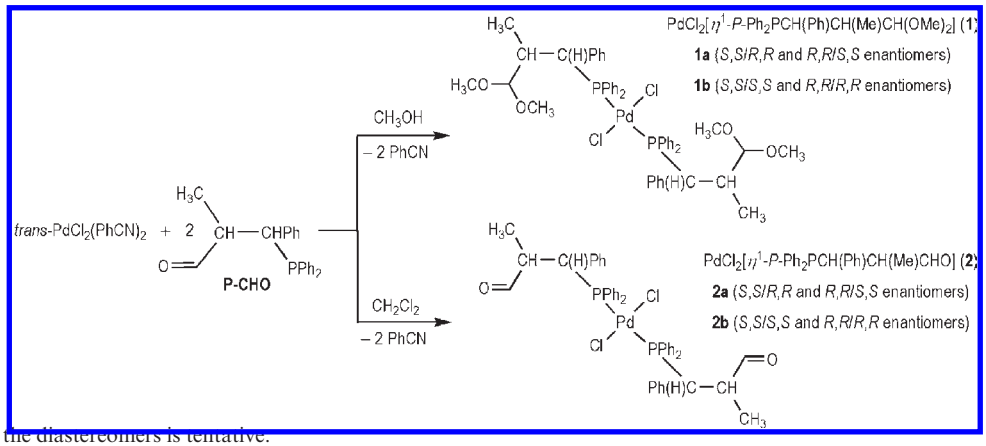

[a] The labeling of the diastereomers is tentative.

Scheme 3. Synthesis of **3** and **4**

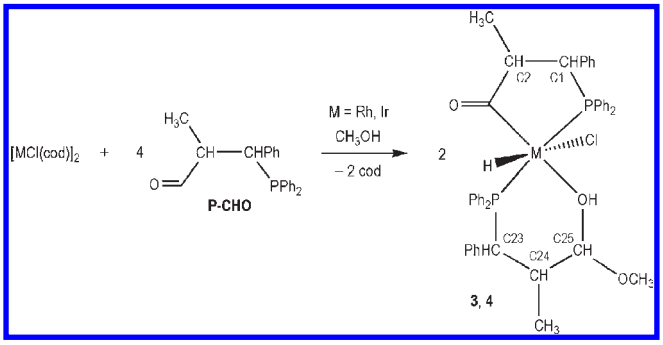

Scheme 4. Equilibrium between the Hemiacetalic and Aldehydic Forms of a **P-CHO** Ligand of **3c** in CD_2Cl_2

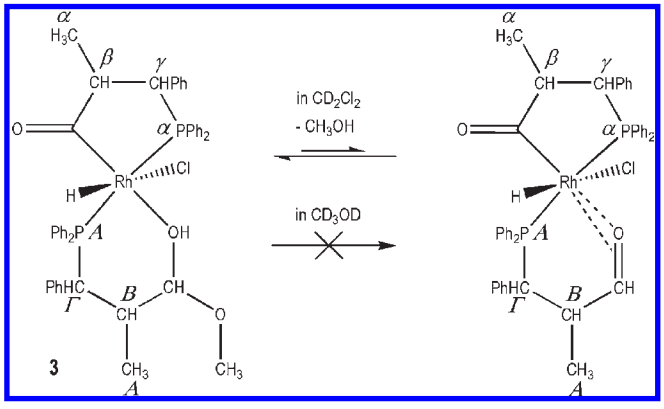

1a (*S*,*S*/*R*,*R* and *R*,*R*/*S*,*S* enantiomers). $^{31}P\{^1H\}$ NMR (CD_2Cl_2): δ 25.20 (s). ^1H NMR (CD_2Cl_2): δ 7.70−6.77 (m, 30H, Ph), 4.70 (dt, 2H, C*H*Ph, $^3J_{HH}$ = 11.3, $^2J_{PH} \approx {}^4J_{PH} \approx 3.6$; $^1H\{^{31}P\}$, d), 3.46 (d, 2H, C*H*(OMe)$_2$ $^3J_{HH}$ = 2.2; $^1H\{^{31}P\}$, same d), 3.14 (s, 6H, OCH_3), 3.07 (s, 6H, OCH_3), 2.63 (m, 2H, C*H*Me), 1.68 (d, 6H, CH_3, $^3J_{HH}$ = 6.8; $^1H\{^{31}P\}$, same d). $^{13}C\{^1H\}$ NMR: δ 137.8 (t, J_{PC} = 2), 136.0 (t, J_{PC} = 5), 135.7 (t, J_{PC} = 6), 131.2 (br s), 130.7 (s), 130.5 (s), 129.4 (t, J_{PC} = 21), 128.3 (s), 127.9 (t, J_{PC} = 5), 127.5 (t, J_{PC} = 5), 127.3 (s), 107.4 (t, *C*H(OMe)$_2$, J_{PC} = 6), 56.9 (s, OCH_3), 55.9 (s, OCH_3), 46.6 (t, P*C*H, J_{PC} = 10), 40.4 (t, *C*HMe, J_{PC} = 2), 14.2 (t, *C*H_3, J_{PC} = 3).

1b (*S*,*S*/*S*,*S* and *R*,*R*/*R*,*R* enantiomers). $^{31}P\{^1H\}$ NMR (CD_2Cl_2): δ 25.35 (s). ^1H NMR (CD_2Cl_2): δ 7.70−6.77 (m, 30H, Ph), 4.69 (dt, 2H, C*H*Ph, $^3J_{HH}$ = 11.3, $^2J_{PH} \approx {}^4J_{PH} \approx 3.6$; $^1H\{^{31}P\}$, d), 3.44 (d, 2H, C*H*(OMe)$_2$, $^3J_{HH}$ = 2.2; $^1H\{^{31}P\}$, same d), 3.13 (s, 6H, OCH_3), 3.07 (s, 6H, OCH_3), 2.63 (m, 2H, C*H*Me), 1.69 (d, 6H, CH_3, $^3J_{HH}$ = 6.8; $^1H\{^{31}P\}$, same d). $^{13}C\{^1H\}$ NMR: δ 137.7 (t, J_{PC} = 2), 136.1 (t, J_{PC} = 5), 135.5 (t, J_{PC} = 6), 131.2 (br s), 130.8 (s), 130.4 (s), 129.6 (t, J_{PC} = 21), 128.3 (s), 127.9 (t, J_{PC} = 5), 127.6 (t, J_{PC} = 5), 127.3 (s), 107.4 (t, *C*H(OMe)$_2$, J_{PC} = 6), 56.8 (s, OCH_3), 55.9 (s), 46.4 (t, P*C*H, J_{PC} = 10), 40.2 (t, *C*HMe, J_{PC} = 2), 14.1 (t, *C*H_3, J_{PC} = 3). [All of the ^1H and $^{13}C\{^1H\}$ signals overlap with the corresponding signals of **1a**].

***trans*-PdCl$_2$[η^1-*P*-(Ph$_2$P)CH(Ph)CH(Me)CHO]$_2$ (2). P-CHO** (87.0 mg, 0.262 mmol) was added to a CH_2Cl_2 solution (~4 mL) of *trans*-$PdCl_2(PhCN)_2$ (50.0 mg, 0.131 mmol)) under Ar at rt and the mixture shaken. After 5 min, 15 mL of Et_2O was added and the mixture volume was reduced to ~2 mL; the resulting precipitated yellow solid was filtered off, washed with Et_2O (~2 mL), and dried under vacuum at 50 °C (70.0 mg, ~64% yield). A satisfactory elemental analysis could not be obtained because of the presence of ~0.2 mol of Et_2O, as revealed by ^1H NMR data in CD_2Cl_2. $^{31}P\{^1H\}$ NMR (CD_2Cl_2): δ 24.95 (s, diastereomer **2a**, see the text), 25.08 s (s, **2b**). ^1H NMR (CD_2Cl_2) for **2a**: δ 9.31 (d, 2H, C*H*O, $^3J_{HH}$ = 2.4; $^1H\{^{31}P\}$, same d), 7.72−6.74 (m, 30H, Ph), 5.00 (m, 2H, C*H*Ph; $^1H\{^{31}P\}$, d, $^3J_{HH}$ = 9.6), 3.30 (m, 2H, C*H*Me), 1.66 (d, 6H, CH_3, $^3J_{HH}$ = 6.8; $^1H\{^{31}P\}$, same d). ^1H NMR data for **2b** were essentially the same as those for **2a**.

Rh(H)Cl[η^2-*P*,*O*H-(Ph$_2$P)CH(Ph)CH(Me)CH(OH)OMe]-[η^2-*P*,*C*(O)-(Ph$_2$P)CH(Ph)CH(Me)C(O)]·MeOH (3·MeOH). The addition of **P-CHO** (20.7 mg, 0.062 mmol) in MeOH (0.5 mL) to a yellow MeOH suspension (0.5 mL) of $[RhCl(COD)]_2$ (7.5 mg, 0.015 mmol) at rt under Ar gave the immediate formation of a pale-yellow solution. X-ray-quality, almost colorless tablet crystals of **3**·MeOH were deposited from the solution within a few hours. The crystals were filtered off, washed with Et_2O (3 × 5.0 mL), and dried in vacuo overnight (8.4 mg, 32%). Satisfactory elemental analyses for nonsolvated **3**, or for the crystal (**3**·MeOH), were not obtained likely because of the variable MeOH content. MS: 800 ($[M - Cl]^+$, where M corresponds to **3**). NMR for isolated crystals (**3**·MeOH, diastereomer **3c**); see the text and Scheme 4 for atom labeling. $^{31}P\{^1H\}$ NMR (CD_2Cl_2): δ 74.84 (dd, P^α, $^1J_{P^\alpha Rh} \approx 137.5$, $^2J_{P^\alpha P^A} \approx 377.7$), 27.49 (dd, P^A, $^1J_{P^A Rh} \approx 135.6$, $^2J_{P^A P^\alpha} \approx 377.7$). ^1H NMR (CD_2Cl_2; see Figure 7): δ 7.91−6.51 (m, 30H, CHC$_6H_5$ and P(C$_6H_5$)$_2$), 4.04 (q, 1H, CH^γ, $^3J_{H^\gamma H^\beta} \cong 6.3$, $^2J_{H^\gamma P^\alpha} \cong 6.0$), 3.99 (dd, 1H, C$H^\Gamma$, $^3J_{H^\Gamma H^B} \approx 5.2$, $^2J_{H^\Gamma P^A} \approx 15.7$), 3.80 (d, $J_{HH} \approx 8.2$), 3.52 (m, $J_{HH} \approx 5.2$), 3.48 (q, 1H, CH^β, $^3J_{H^\beta H^\alpha} \approx {}^3J_{H^\beta H^\gamma} \approx 6.6$), 2.99 (q, 1H, C$H^B$, $^3J_{H^B H^A} \approx {}^3J_{H^B H^\Gamma} \approx 5.0$−7.0), 1.23 (d, 3H, C$H^A{}_3$, $^3J_{H^A H^B} \approx 6.9$), 0.88 (d, 3H, C$H^\alpha{}_3$, $^3J_{H^\alpha H^\beta} \approx 6.7$), −14.43 (ddd, 1H, Rh*H*, $^1J_{HRh} \approx 26.3$, $^2J_{HP^{\alpha/A}} \approx 12.1$, $^2J_{HP^{A/\alpha}} \approx 8.5$). $^{13}C\{^1H\}$ NMR (CD_2Cl_2): δ 136.32−127.46 (CHC$_6H_5$ and P(C$_6H_5$)$_2$), 61.81 (s, C$^\beta$), 46.85 (s, C$^\gamma$), 45.37 (s, C^B), 18.57 (s, C^A), 14.56 (s, C$^\alpha$). See the text and Table 1, and Table S1 in the Supporting Information for

Table 1. $^{31}P\{^1H\}$ NMR Data,[a] and ^1H and $^1H\{^{31}P\}$ NMR Data for the Hydride Region, for Diastereomers of **3**

	δ_{P^A}	δ_{P^α}	J_{P^ARh}	$J_{P^\alpha Rh}$	$J_{P^AP^\alpha}$	δ_{RhH}	^1H signal	$^1H\{^{31}P\}$ signal	J_{HRh}	J_{HP^α} or J_{HP^A}	
3a[b]	34.50	71.53	132.8	136.2	380.7	−14.65	m	br d	26.7		
3b[b]	41.67	73.21	134.0	141.7	371.6	−13.98	ddd	d	25.9	6.6	10.2
3b[c]	40.72	72.52	135.0	139.0	376.4	−13.44	ddd	d	26.1	6.3	10.3
3c[c]	27.49	74.84	135.6	137.5	377.7	−14.43	ddd	d	26.3	12.1	8.5

[a] $^{31}P\{^1H\}$ NMR signals are all dd; *J* values are in Hertz. [b] In situ species seen in CD_3OD. [c] Isolated complex in CD_2Cl_2.

Table 2. $^{31}P\{^1H\}$ NMR Data,[a] and ^1H and $^1H\{^{31}P\}$ NMR Data for the Hydride Region, for Diastereomers of **4**

	δ_{P^A}	δ_{P^α}	$J_{P^AP^\alpha}$	δ_{IrH}	$J_{HP^\alpha} \cong J_{HP^A}$
4a[b]	21.84	47.00	376.0	−17.93	13.7
4a[c]	22.81	48.57	371.4	−17.30	14.0
4b[b]	24.69	49.12	366.1	−18.38	14.7
4c[b]	23.69	49.66	366.9	−17.97	13.9

[a] $^{31}P\{^1H\}$ NMR signals are d; ^1H and $^1H\{^{31}P\}$ NMR signals are t and s, respectively; *J* values are in Hertz. [b] In situ species seen in CD_3OD. [c] Isolated complex in CD_2Cl_2.

NMR data of other diastereomers. IR (Nujol): 1619 ($\nu_{C=O}$), 2047 (ν_{Rh-H}). IR (CH_2Cl_2): 1652 ($\nu_{C=O}$), 2004 (ν_{Rh-H}).

Ir(H)Cl[η^2-*P*,*O*H-(Ph_2P)CH(Ph)CH(Me)CH(OH)OMe][η^2-*P*,*C*(O)-(Ph_2P)CH(Ph)CH(Me)C(O)]·MeOH (4·MeOH). The addition of **P-CHO** (20.3 mg, 0.06z1 mmol) in MeOH (0.5 mL) to a red, MeOH suspension (0.5 mL) of $[IrCl(COD)]_2$ (10.0 mg, 0.015 mmol) at rt under Ar gave the immediate formation of a pale-yellow solution, from which X-ray-quality, almost colorless crystals of **4**·MeOH were deposited; these were filtered off, washed with Et_2O (3 × 5.0 mL), and dried in vacuo overnight (13.8 mg, 24%). Satisfactory elemental analysis for the crystal was not obtained likely because of the presence of an impurity (see Figure S5 in the Supporting Information). MS: 889 ($[M - Cl]^+$, where M corresponds to **4**). NMR: see the text, Table 2, and Figure 9 for atom labeling. $^{31}P\{^1H\}$ NMR (CD_3OD): for **4a**, δ 47.00 (d, $P^\alpha Ph_2$, $^2J_{P^\alpha P^A} \approx 376.0$), 21.84 (d, $P^A Ph_2$, $^2J_{P^AP^\alpha} \approx 376.0$); for **4b**, δ 49.12 (d, $P^\alpha Ph_2$, $^2J_{P^\alpha P^A} \approx 366.1$), 24.69 (d, $P^A Ph_2$, $^2J_{P^AP^\alpha} \approx 366.1$); for **4c**, δ 49.66 (d, $P^\alpha Ph_2$, $^2J_{P^\alpha P^A} \approx 366.9$), 23.69 (d, $P^A Ph_2$, $^2J_{P^AP^\alpha} \approx 366.9$). $^{31}P\{^1H\}$ NMR (CD_2Cl_2): for **4a**, δ 48.57 (d, $P^\alpha Ph_2$, $^2J_{P^\alpha P^A} \approx 371.4$), 22.81 (d, $P^A Ph_2$, $^2J_{P^AP^\alpha} \approx 371.4$). ^1H NMR (CD_3OD): for **4a**, δ −17.93 (t, 1H, Ir*H*, $^2J_{HP^{\alpha/A}} \approx {}^2J_{HP^{A/\alpha}} \approx 13.7$); for **4b**, δ −18.38 (t, 1H, Ir*H*, $^2J_{HP^{\alpha/A}} \approx {}^2J_{HP^{A/\alpha}} \approx 14.7$); for **4c**, δ −17.97 (t, 1H, Ir*H*, $^2J_{HP^{\alpha/A}} \approx {}^2J_{HP^{A/\alpha}} \approx 13.9$). ^1H NMR (CD_2Cl_2): for **4a**, δ −17.30 (t, 1H, Ir*H*, $^2J_{HP^{\alpha/A}} \approx {}^2J_{HP^{A/\alpha}} \approx 14.0$). IR (Nujol): 1639 ($\nu_{C=O}$), 2033 ($\nu_{Rh-H}$). IR ($CH_2Cl_2$): 1633 ($\nu_{C=O}$), 2004 ($\nu_{Rh-H}$).

X-ray Analysis of 1, 3·MeOH, and 4·MeOH, as Diastereomers 1a, 3c, and 4a, Respectively. Measurements were made at 173 (±0.1) K on a Bruker X8 APEX diffractometer using graphite-monochromated Mo Kα radiation (0.71073 Å). Data were collected and integrated using the Bruker *SAINT* software package[10] and were corrected for absorption effects using a multiscan technique (*SADABS*),[11] with minimum and maximum transmission coefficients of 0.707 and 0.969 for **1a**, 0.817 and 0.913 for **3c**, and 0.563 and 0.705 for **4a**, respectively. The data were corrected for Lorentz and polarization effects, and the structures were solved by direct methods.[12] Some crystallographic data and selected bond lengths and angles for the complexes are given in Tables 3 and 4.

(10) *SAINT*, version 7.03A; Bruker AXS Inc.: Madison, WI, **1997**−**2003**.
(11) *SADABS, Bruker Nonius area detector scaling and absorption correction*, version 2.10; Bruker AXS Inc.: Madison, WI, **2003**.
(12) Altomare, A.; Burla, M. C.; Camalli, M.; Cascarano, G. L.; Giacovazzo, C.; Guagliardi, A.; Moliterni, A. G. G.; Polidori, G.; Spagna, R. *J. Appl. Crystallogr.* **1999**, *32*, 115.

Results and Discussion

As noted in the Introduction, the phosphine **P-CHO** used for syntheses of the complexes was a mixture of diastereomers in a dr ratio of ∼20 [or, in the less preferred nomenclature,[13] a diastereomeric excess (de) value of 91%], with the major diastereomer being a mixture of the *S*,*S*/*R*,*R* enantiomers.[1] This phosphine, although having two chiral centers [versus one, for example, in (Ph_2P)CH(Ph)CH_2CHO],[1] was selected for study because of the crystalline products generated with the Pd, Rh, and Ir precursors.

Dissolution of **P-CHO** in MeOH/CD_3OD at rt generates the hemiacetal. The $^{31}P\{^1H\}$ data (Figure 1) reveal that a slow equilibrium is established between **P-CHO** and the hemiacetal, which has a third chiral center that is generated in the *R* and *S* forms within a mixture of diastereomers (δ_P −3.31 and −5.26); after 18 h, the hemiacetal/aldehyde equilibrium ratio is ∼3.3, and dr is ∼1.1 for the hemiacetal diastereomers. We have shown recently that (Ph_2P)CH(Ph)CH_2CHO, when dissolved in MeOH, similarly generates the hemiacetal.[14] The aldehyde/hemiacetal equilibrium, however, does not appear to be important in the metal complex syntheses that were carried out in MeOH: the findings imply that these reactions involve the *S*,*S*/*R*,*R* enantiomers of **P-CHO** and that the metal plays a role in subsequent conversions to a coordinated hemiacetal ligand (with Rh and Ir) or coordinated acetal ligand (with Pd); see below.

Palladium Systems. The rt 2:1 reaction of **P-CHO** with *trans*-$PdCl_2(PhCN)_2$ in MeOH slowly precipitated yellow crystals of **1** in 66% yield; X-ray and NMR data show that the −CHO moiety has now been converted into −$CH(OMe)_2$, an acetal group. The X-ray data reveal that **1** (as diastereomer **1a**; see below) crystallizes with two crystallographically racemic half-molecules residing on two separate inversion centers. The structure (Figure 2) shows a typical square-planar Pd^{II} complex, and the bond lengths and angles at the metal are very similar to those found in such *trans*-dichlorobis(phosphine)palladium(II) complexes,[15] with an average Pd−Cl bond length of 2.31 Å and an average Pd−P bond length of 2.33 Å; the P−Pd−Cl angles of 85.46−86.84° and 93.16−94.54° reveal a slight distortion of the square-planar geometry.

(13) Gawley, R. E. *J. Org. Chem.* **2006**, *71*, 2411.
(14) Moiseev, D. V.; Marcazzan, P.; James, B. R. *Can. J. Chem.* **2009**, *87*, 582.
(15) (a) Grossman, O.; Azerraf, C.; Gelman, D. *Organometallics* **2006**, *25*, 375. (b) Baber, R. A.; Orpen, A. G.; Pringle, P. G.; Wilkinson, M. J.; Wingad, R. L. *J. Chem. Soc., Dalton Trans.* **2005**, 659. (c) Stott, T. L.; Wolf, M. O.; Lam, A. *J. Chem. Soc., Dalton Trans.* **2005**, 652. (d) Ronig, B.; Schulze, H.; Pantenburg, I.; Wesemann, L. *Eur. J. Inorg. Chem.* **2005**, 314. (e) Yamamoto, Y.; Sinozuka, Y.; Tsutsumi, Y.; Fuse, K.; Kuge, K.; Sunada, Y.; Tatsumi, K. *Inorg. Chim. Acta* **2004**, *357*, 1270. (f) Carlson, S. J.; Lu, T.; Luck, R. L. *Inorg. Chem. Commun.* **2003**, *6*, 455. (g) Ogasawara, M.; Yoshida, K.; Hayashi, T. *Organometallics* **2001**, *20*, 1014.

Table 3. Crystal Data for Complexes **1** (as Diastereomer **1a**), **3**·MeOH (as **3c**), and **4**·MeOH (as **4a**)

	diastereomer **1a**	diastereomer **3c**	diastereomer **4a**
empirical formula	$C_{48}H_{54}O_4P_2PdCl_2$	$C_{46}H_{50}O_4P_2RhCl$	$C_{46}H_{50}O_4P_2IrCl$
fw	934.15	867.16	956.45
cryst syst	triclinic	triclinic	triclinic
space group	$P\bar{1}$ (No. 2)	$P\bar{1}$ (No. 2)	$P\bar{1}$ (No. 2)
cryst size (mm^3)	0.05 × 0.10 × 0.20	0.15 × 0.25 × 0.35	0.10 × 0.10 × 0.30
a (Å)	10.0267(10)	9.4745(9)	9.4305(7)
b (Å)	12.5501(9)	13.1717(14)	13.2091(9)
c (Å)	18.985(2)	17.0833(18)	17.0558(10)
α (deg)	79.087(3)	103.924(6)	103.965(3)
β (deg)	76.743(3)	91.575(6)	91.563(3)
γ (deg)	88.483(3)	100.780(6)	100.752(3)
volume ($Å^3$)	5220.68(5)	2026.9(4)	2019.8(2)
Z	2	2	2
D_{calcd} ($mg\ m^{-3}$)	1.359	1.421	1.573
μ (mm^{-1})	0.635	0.610	3.494
$F(000)$	968.00	900.00	964.00
reflns collcd	18 265	48 876	36 216
unique reflns [R(int)]	5911 [0.087]	9701 [0.049]	9205 [0.047]
no. of variables	523	503	497
GOF on F^2	1.00	1.04	1.16
final R indices [$I > 2\sigma(I)$]	R1 = 0.118[a]; wR2 = 0.112[b]	R1 = 0.042[a]; wR2 = 0.067[b]	R1 = 0.066[a]; wR2 = 0.115[b]
max differential peak/hole (e $Å^{-3}$)	0.48/−0.47	0.41/−0.45	3.78/−1.72

[a] $R1 = \sum||F_o| - |F_c||/\sum|F_o|$. [b] $wR2 = [\sum(w(F_o^2 - F_c^2)^2)/\sum w(F_o^2)^2]^{1/2}$.

The structural data show that **1** crystallizes as one diastereomer (labeled **1a**), with enantiomeric configurations *S*,*S*/*R*,*R* and *R*,*R*/*S*,*S* of the coordinated, chiral phosphine molecules; other diastereomers are not observed in the solid state. The immediately measured ^1H and $^{31}P\{^1H\}$ NMR spectra of **1a** dissolved in CD_2Cl_2 are consistent with this: the $^{31}P\{^1H\}$ spectrum (Figure 3) reveals a major resonance at δ_P 25.20, attributed to **1a**, along with trace resonances at δ_P 25.35, 24.65, and 23.95, considered due to the presence of minor amounts of other diastereomers (the trace δ_P 25.35 signal is discussed below).[16] The ^1H NMR resonance for the C*H*Ph protons of **1a** appears as a doublet of triplets centered at δ_H 4.70, which collapses into a doublet in the $^1H\{^{31}P\}$ NMR spectrum ($^3J_{HH}$ = 11.3), with the dt pattern implying that $^2J_{PH} \approx {}^4J_{PH} \approx 3.6$. The resonance of the C*H*(OMe)$_2$ proton is a doublet at δ_H 3.46 ($^3J_{HH}$ = 2.2) in both the ^1H and $^1H\{^{31}P\}$ NMR spectra, while the peaks due to the diastereotopic −OMe groups are singlets at δ_H 3.14 and 3.07.

The intensity of the trace signal at δ_P 25.35 increases with time (Figure 3) and is attributed to a second diastereomer, **1b** (possibly the *S*,*S*/*S*,*S* and *R*,*R*/*R*,*R* enantiomers), with the intensities of the **1a** and **1b** δ_P signals becoming equal after 2 days. The ^1H and $^{13}C\{^1H\}$ NMR data of **1b** are essentially identical with those of **1a**. Several triplets are seen in the $^{13}C\{^1H\}$ NMR spectra of **1a** and **1b**, presumably because of a virtual coupling between the two *trans*-P atoms;[17] the $^{13}C\{^1H\}$ NMR resonances are assigned except for the aromatic C atoms. The mechanism of the slow equilibration among the two diastereomers has not been studied, but, of note, no free **P-CHO** was detected in solution; this does not rule out its role in stereoconversion, and other mechanisms involving bridging of the free aldehyde or acetal ends of initially monodentate ligands between two Pd centers are possible.

When the 2:1 reaction of **P-CHO** with *trans*-$PdCl_2(PhCN)_2$ is carried out in CH_2Cl_2, a pale-yellow solution is formed immediately, and isolation of **2** (in ∼64% yield) required the addition of Et_2O; in this system, of course, the phosphine CHO group remains as such (as detected in the ^1H NMR spectra). The in situ $^{31}P\{^1H\}$ NMR spectrum of the yellow solution shows equal-intensity singlets at δ_P 24.95 and 25.08, as well as four other trace peaks (Figure S1 in the Supporting Information).[16] The $^{31}P\{^1H\}$ NMR spectrum of isolated **2** dissolved in CD_2Cl_2 shows immediately the same two major singlets, but with an intensity ratio of ∼3:1 that changes over 3 h to a 1:1 intensity; the signals are assigned, respectively, to diastereomers **2a** (presumably preferred in the solid state) and **2b**, with the same tentative configurations as those shown for **1a** and **1b** (see Scheme 2). The ^1H NMR data for each diastereomer are almost identical. Thus, the −C*H*O protons appear as a doublet in the ^1H and $^1H\{^{31}P\}$ NMR spectra at δ_H 9.31 ($^3J_{HH}$ = 2.5) for both **2a** and **2b** [the δ_H value is shifted to a higher field than that of **P-CHO** (δ_H 9.97)]; the C*H*Ph resonance appears as a multiplet centered at δ_H 5.00, which collapses in the $^1H\{^{31}P\}$ NMR spectrum into two doublets ($^3J_{HH}$ = 9.6, $\Delta\delta$ = 4 Hz), one for each diastereomer; the C*H*Me and C*H*$_3$ resonances appear as a multiplet and a doublet at δ_H 3.30 and 1.66, respectively, for both **2a** and **2b**. Over several days, the immediate in situ $^{31}P\{^1H\}$ NMR spectrum, and that of CD_2Cl_2 solutions of isolated **2**, became much more complex, with further signals appearing in the δ_P 6−8 and 24−28 regions, presumably because of the formation of other diastereomers.

Rhodium Systems. The rt reaction of $[RhCl(COD)]_2$ in MeOH with **P-CHO** (phosphine:Rh = 2) is shown in Scheme 3, with the crystallographic data of an isolated diastereomer (**3c**) providing the crucial information (see below). Mixing of the reagents immediately gave a yellow solution, which was studied by in situ $^{31}P\{^1H\}$ and

(16) Diastereomers formed from the minor (9%) form of **P-CHO** with the Pd^{II}, Rh^{III}, and Ir^{III} complexes are not detectable in NMR spectra of the isolated complexes, but their existence in in situ systems cannot be ruled out (e.g., see, Figure S1 in the Supporting Information).

(17) (a) Bovey, F. A. *Nuclear Magnetic Resonance Spectroscopy*; Academic Press: New York, 1969; p 11. (b) Jenkins, J. M.; Shaw, B. L. *Proc. Chem. Soc., London* **1963**, 279.

Table 4. Selected Bond Lengths (Å) and Angles (deg) in **1a**, **3**·MeOH (**3c**), and **4**·MeOH (**4a**)

1a[a]	Pd1−Cl1	2.3126(16)	C3−H3	1.0000
	Pd1−P1	2.3207(17)	C3−O1	1.392(8)
	C3−C2	1.534(9)	C3−O2	1.423(8)
	Cl1−Pd1−P1	94.54(6)	C2−C3−O2	110.1(6)
	Cl1−Pd1−P1*	85.46(6)	H3−C3−O1	110.0
	C2−C3−H3	110.0	H3−C3−O2	110.0
	C2−C3−O1	107.3(6)	O1−C3−O2	109.3(6)
3c	Rh1−C3	1.9548(19)	C25−C24	1.515(3)
	Rh1−Cl1	2.4290(5)	C25−H25	1.0000
	Rh1−H	1.511(19)	C25−O2	1.421(2)
	Rh1−O2	2.2726(14)	C25−O3	1.403(2)
	Rh1−P1	2.2765(6)	O2−H20	0.78(2)
	Rh1−P2	2.3522(5)	O4...H20	1.84(3)
	C3−O1	1.219(2)	O4···O2	2.614(2)
	C3−Rh1−Cl1	94.58(5)	O1−C3−Rh1	123.40(15)
	C3−Rh1−H	87.5(8)	P1−Rh1−P2	171.211(18)
	C3−Rh1−O2	176.10(6)	Rh1−P1−C1	101.75(6)
	C3−Rh1−P1	85.16(6)	P1−C1−C2	103.46(13)
	C3−Rh1−P2	93.34(6)	C1−C2−C3	111.77(15)
	Cl1−Rh1−H	177.8(8)	C2−C3−Rh1	118.48(13)
	Cl1−Rh1−O2	89.26(4)	C24−C25−H25	109.6
	Cl1−Rh1−P1	94.575(19)	C24−C25−O2	109.74(15)
	Cl1−Rh1−P2	94.177(19)	C24−C25−O3	107.00(15)
	H−Rh1−O2	88.6(8)	H25−C25−O2	109.6
	H−Rh1−P1	86.1(7)	H25−C25−O3	109.6
	H−Rh1−P2	85.2(7)	O2−C25−O3	111.28(15)
	O2−Rh1−P1	95.25(4)	O4···H20−O2	172(3)
	O2−Rh1−P2	85.67(4)		
4a	Ir1−C3	1.961(6)	C25−C24	1.521(9)
	Ir1−Cl1	2.4374(17)	C25−H25	1.0000
	Ir1−H	1.6774(3)	C25−O2	1.428(8)
	Ir1−O2	2.261(4)	C25−O3	1.390(8)
	Ir1−P1	2.2817(17)	O2−H20	0.87(8)
	Ir1−P2	2.3406(17)	O4···H20	1.81(8)
	C3−O1	1.212(8)	O4···O2	2.586(7)
	C3−Ir1−Cl1	95.1(2)	O1−C3−Ir1	124.2(5)
	C3−Ir1−H	98.9(2)	P1−Ir1−P2	172.34(6)
	C3−Ir1−O2	177.0(2)	Ir1−P1−C1	102.1(2)
	C3−Ir1−P1	85.3(2)	P1−C1−C2	103.3(5)
	C3−Ir1−P2	92.9(2)	C1−C2−C3	112.5(5)
	Cl1−Ir1−H	165.99(4)	C2−C3−Ir1	118.0(5)
	Cl1−Ir1−O2	87.74(13)	C24−C25−H25	109.8
	Cl1−Ir1−P1	94.20(6)	C24−C25−O2	109.4(5)
	Cl1−Ir1−P2	93.36(6)	C24−C25−O3	106.8(6)
	H−Ir1−O2	78.28(12)	H25−C25−O2	109.8
	H−Ir1−P1	88.23(5)	H25−C25−O3	109.8
	H−Ir1−P2	84.73(4)	O2−C25−O3	111.3(6)
	O2−Ir1−P1	95.74(12)	O4···H20−O2	148(8)
	O2−Ir1−P2	85.77(12)		

[a] Data for one of the two molecules in the asymmetric unit.

^{1}H NMR spectra; these revealed the presence of some unreacted **P-CHO** with small amounts in the hemiacetal form (see Figure 1), free COD (δ_H 2.33, br m; 5.51, br m), and the complex **3**. That is, one **P-CHO** is chelated via the P and O atoms of the hemiacetal (η^2-*PO*^{OH}; Scheme 1e), while in a second **P-CHO**, the −CHO moiety has undergone oxidative addition to form a hydridoacyl species (H,η^2-*PC*; Scheme 1b). As noted above, the free **P-CHO**/hemiacetal equilibrium is slow (Figure 1), and thus the metal must promote the hemiacetal formation. The closest analogy to this Rh chemistry is the reported reaction in benzene of *o*-diphenylphosphinobenzaldehyde with Rh^I precursors, which generates a species analogous to **3** but in

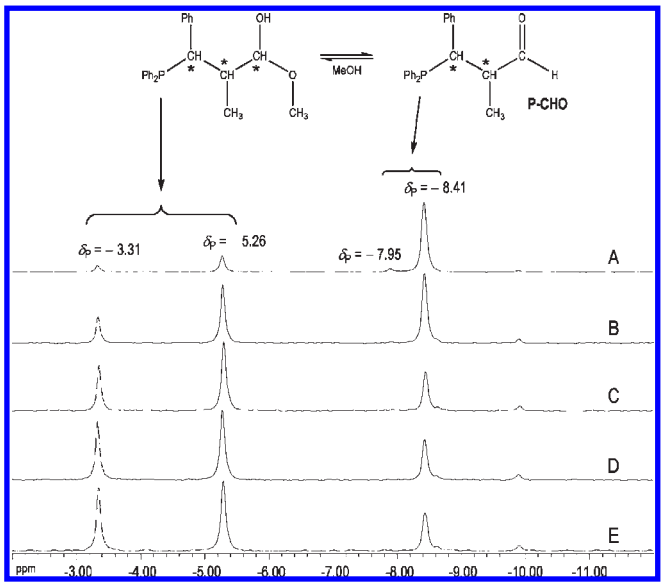

Figure 1. ^{31}P{^{1}H} NMR spectra of a CD_3OD solution of **P-CHO** after (A) 20 min, (B) 1.5 h, (C) 3.5 h, (D) 6 h, and (E) 18 h. Asterisks represent chiral centers; the major (*S*,*S*/*R*,*R*) and minor (*S*,*R*/*R*,*S*) diastereomers of **P-CHO** are seen at δ_P −8.41 and −7.95, respectively.

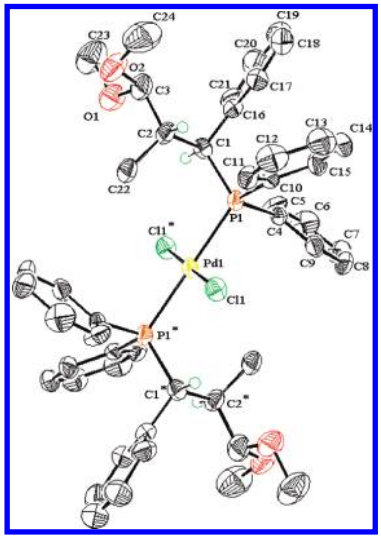

Figure 2. Crystal structure of **1** (diastereomer **1a**), with 50% probability ellipsoids.

which the "lower" **P-CHO** ligand (cf. Scheme 3) is bonded via the P atom and the aldehyde O atom.[2a,3f,4a]

The hemiacetal formation results in an additional chiral center (C25) in type **3** species which thus contain five chiral centers, namely, C1, C2, C23, C24, and C25, as shown in Scheme 3 and the labeled crystal structure (Figure 4). Theoretically, many diastereomers exist, but ^{31}P{^{1}H} NMR data show that only two are detected in the in situ formation of **3** in a CD_3OD solution (Figure 5). Two doublet of doublets at δ_P 34.50 (J_{P^ARh} = 132.8, $J_{P^AP^\alpha}$ = 380.7) and 71.53 ($J_{P^\alpha Rh}$ = 136.2, $J_{P^\alpha P^A}$ = 380.7) are assigned to the major diastereomer **3a**, and two doublet of doublets at δ_P 41.67 (J_{P^ARh} = 134.0, $J_{P^AP^\alpha}$ = 371.6) and 73.21 ($J_{P^\alpha Rh}$ = 141.7, $J_{P^\alpha P^A}$ = 371.6) are assigned to diastereomer **3b** (Table 1). The **3a**:**3b** ratio of ∼2:1 does not change for ∼2 h, when diastereomer **3c**

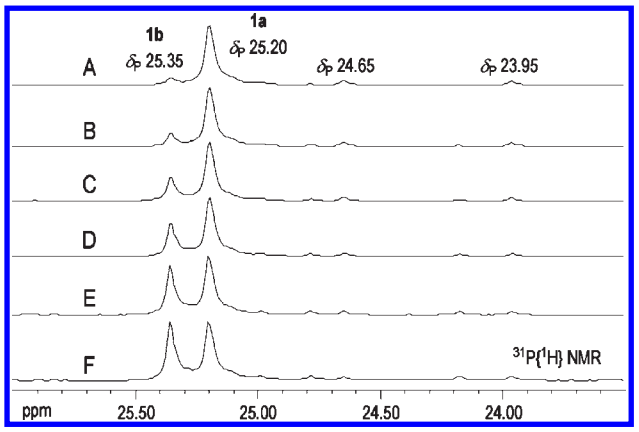

Figure 3. $^{31}P\{^1H\}$ NMR spectrum of a CD_2Cl_2 solution of isolated **1a** after (A) 15 min, (B) 3 h, (C) 7.5 h, (D) 12.5 h, (E) 24 h, and (F) 48 h.

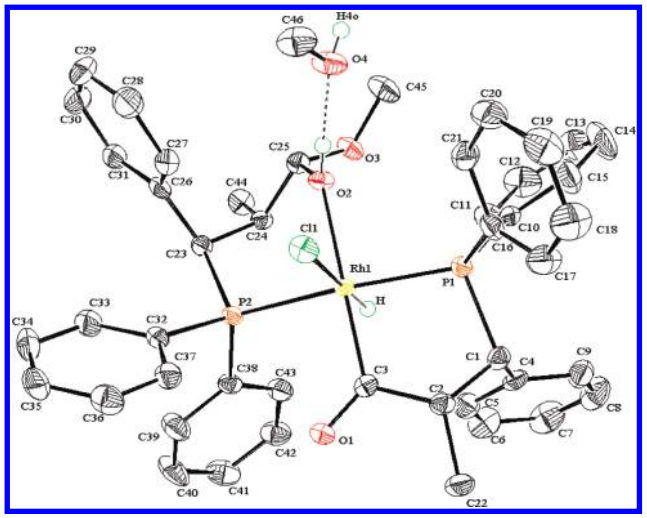

Figure 4. Crystal structure of **3**·MeOH (diastereomer **3c**), with 50% probability ellipsoids.

starts to precipitate (see below). The $^{31}P\{^1H\}$ NMR data are consistent with the literature data[18] in that the formation of a five-membered ring results in the lower-field signal for P^{α} of the phosphine ligand (with a higher-field signal being observed for P^{A} in the six-membered, hemiacetal ring); large $J_{P^{\alpha}P^{A}}$ coupling constants define mutually *trans*-P atoms, and the $J_{P^{A}Rh}$ and $J_{P^{\alpha}Rh}$ values are in the typically reported range.

Species **3a** and **3b** (presumably the most energetically favored diastereomers) are conceivably epimers that differ just in the stereochemistry of the C25 hemiacetal C atom, and once formed, further rearrangement at C25 is unlikely in MeOH (see Scheme 4). A different behavior is seen when CD_2Cl_2 solutions of the isolated crystalline complex **3**·MeOH are monitored (see below). Once the spontaneous precipitation of the almost colorless crystals begins in MeOH (32% yield), the intensities of the $^{31}P\{^1H\}$ NMR signals of **3a** and **3b** (Figure 5) slowly decrease. The insolubility of a new diastereomer (**3c**) in MeOH must account for its eventual, favored formation. The elemental analysis determined for the crystalline **3**·MeOH (**3c**) was unsatisfactory, but $^{31}P\{^1H\}$ NMR data (Figures 5 and 6) show the absence of any P-containing impurities. Essentially identical findings were found for a 1:1 Rh/**P-CHO** reaction in MeOH: "immediate" in situ NMR revealed the presence of the 2:1 ratio of **3a** and **3b**, with subsequent slow precipitation of crystals of **3c**.

The crucial crystallographic data revealing the two bonding modes of the reactant **P-CHO** were obtained on **3c**. The asymmetric unit contains two almost identical, independent molecules, of which one is shown in Figure 4. MeOH is bound via a strong hydrogen bond between the O atom of MeOH and the hydroxyl H atom of the hemiacetal group (O4···H2o = 1.84 Å). Within the asymmetric unit, there are three more intermolecular O···H bonds for each of the two independent MeOH molecules: one strong one (O···H = 1.94 Å) between the acyl O atom and the hydroxyl H atom H2o of a second MeOH molecule, a weaker one (O···H = 2.49 Å) between the O atom of MeOH and the H atom H21 of a PPh_2-phenyl ring within the η^2-acylphosphine, and a marginal one (O···H = 2.76 Å) between the hydroxyl H atom H2o of MeOH and an acyl O atom of a second molecule of the complex. Other comments on the geometrical parameters will be considered along with those on the analogous Ir complex (see below).

The structure reveals that **3c** crystallizes as one diastereomer present in two enantiomeric forms: the relative configurations of the C atoms C1, C2, C23, C24, and C25 are *S*,*R*,*S*,*R*,*R* (called enantiomer **3c**-E1) and *R*,*S*,*R*, *S*,*S* (**3c**-E2). The two independent molecules of the asymmetric unit represent **3c**-E1 and **3c**-E2 (Figure S2-A in the Supporting Information), which are indistinguishable by NMR spectroscopy; thus, the $^{31}P\{^1H\}$ NMR spectrum of a freshly prepared CD_2Cl_2 solution of **3c** (Figure 6) shows only two doublet of doublets at δ_P 27.49 ($J_{P^{A}Rh}$ = 135.6, $J_{P^{A}P^{\alpha}}$ = 377.7) and 74.84 ($J_{P^{\alpha}Rh}$ = 137.5, $J_{P^{\alpha}P^{A}}$ = 377.7) (see the Experimental Section and Table 1). The hydride ligand of **3c** was located by X-ray analysis, solid-state and solution IR (which also reveals $\nu_{C=O}$ of the acyl moiety), and ^1H NMR data in CD_2Cl_2 solution as a high-field doublet of doublets of doublets, which collapses to a doublet in $^1H\{^{31}P\}$ NMR spectra (Table 1 and Figure S3 in the Supporting Information); this figure also shows trace amounts of **3b** and another diastereomer. Over 22 h, **3c** converts to **3b**, which is the favored diastereomer in CD_2Cl_2 (Table 1 and Figure S4 in the Supporting Information), and during this period, small amounts of other diastereomers (**3d**−**3j**) are also detected and similarly characterized (e.g., see Figure S4 and Table S1 in the Supporting Information); **3h**−**3j** were only detected in the more sensitive ^1H and $^1H\{^{31}P\}$ NMR spectra.

Measurement of ^1H, $^1H\{^{31}P\}$, 2D HSQC $^{31}P\{^1H\}/^1H$, and 2D HSQC and HMBC $^{13}C\{^1H\}/^1H$ NMR spectra in CD_2Cl_2 allowed for the assignment of the ^1H and ^{13}C NMR resonances of the aliphatic C and H atoms of **3c** (see the Experimental Section), although there is some uncertainty regarding the coordinated hemiacetal −CH(OH)OMe group because of an associated hemiacetal/aldehyde equilibrium to be discussed below. The relevant ^1H NMR signals of the hemiacetal group are broadened and are present in the δ_H 2.94−4.08 region (Figure 7),

(18) (a) Lorenzini, F.; Patrick, B. O.; James, B. R. *Inorg. Chem.* **2007**, *46*, 8998. (b) Cipot, J.; McDonald, R.; Ferguson, M. J.; Schatte, G.; Stradiotto, M. *Organometallics* **2007**, *26*, 594. (c) Han, L.-B.; Tilley, T. D. *J. Am. Chem. Soc.* **2006**, *128*, 13698. (d) Marcazzan, P.; Patrick, B. O.; James, B. R. *Organometallics* **2005**, *24*, 1445. (e) Raebiger, J. W.; DuBois, D. L. *Organometallics* **2005**, *24*, 110. (f) Merckle, C.; Blümel, J. *Top. Catal.* **2005**, *34*, 5.

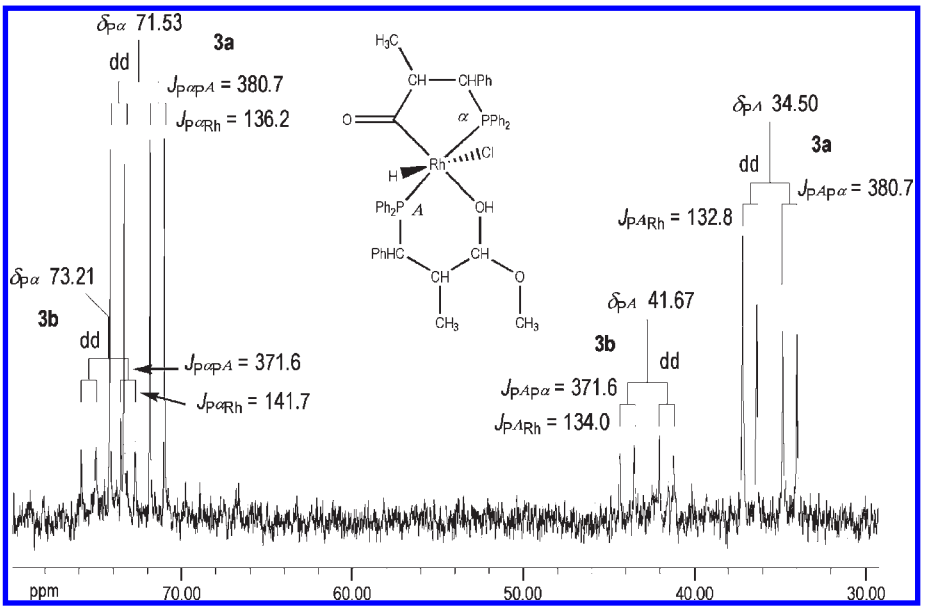

Figure 5. In situ $^{31}P\{^{1}H\}$ NMR spectrum of a CD_3OD solution of **3**, showing two diastereomers **3a** and **3b** (**3a**:**3b** ~ 2:1).

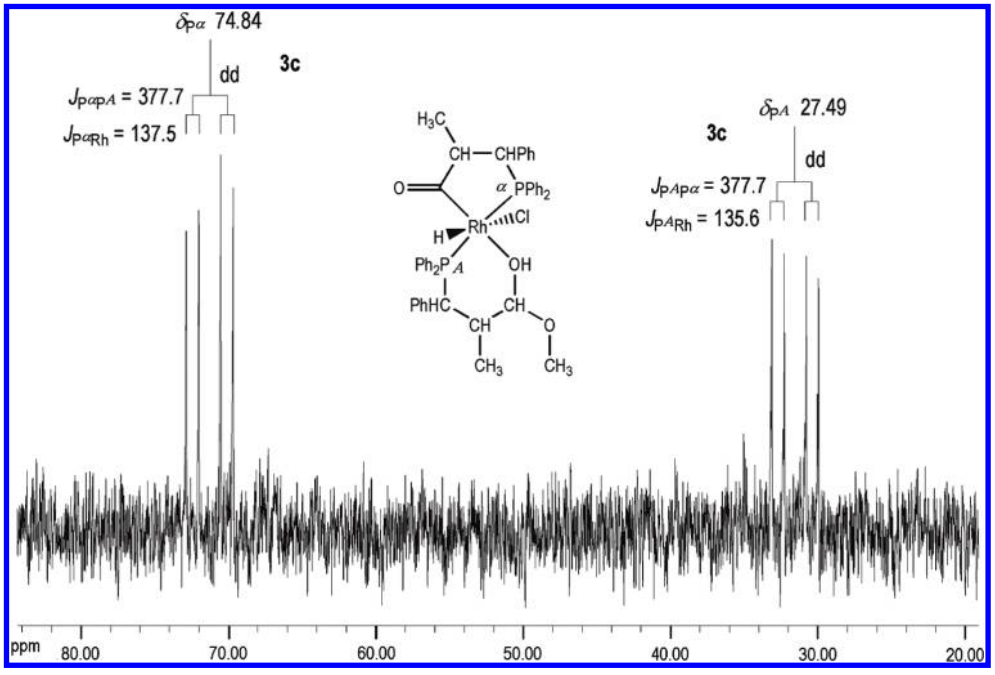

Figure 6. $^{31}P\{^{1}H\}$ NMR spectrum of a freshly prepared CD_2Cl_2 solution of **3**·MeOH, isolated as diastereomer **3c**.

where the integration accounts for the four methylenic protons [quintets at δ_H 2.99 (H^B), 3.48 (H^β), and 4.04 (H^γ) and a doublet of doublets at δ_H 3.99 (H^Γ)] *and* the five protons of −CH(OH)OMe. A doublet at δ_H 3.80 (J_{HH} = 8.2) and a multiplet at δ 3.52, with the latter overlapping with the H^β quintet, account for the two C*H*(O*H*) protons, but their mutual assignments cannot be made definitively; however, the methylenic proton is considered more likely to give rise to the multiplet. [It should be noted that within complexes containing an Rh−OH moiety coupling of the alcohol (or phenol) proton to the Rh has not been observed.[19]] The required 30 aromatic protons fall in the range of δ_H 6.51−7.91. The $^{13}C\{^{1}H\}$ NMR resonances for the −CH(OH)OMe moiety were not detected, presumably because of the hemiacetal/aldehyde equilibrium; however, even the aromatic carbon signals were weak after running the spectrum for ~12 h. The expected Rh-*C*O signal was also not definitively assigned, although a very weak broad signal centered at δ ~185 might be this resonance; further, it is possible that the η^2-acylphosphine ligand is involved in some labile processes that could play a role in the formation of the various diastereomers.

The behavior of aging solutions of isolated **3c** in CD_2Cl_2 is noteworthy and quite different from that

(19) (a) Lahuerta, P.; Moreno, E.; Monge, A.; Muller, G.; Pérez-Prieto, J.; Sanaú, M.; Stiriba, S.-E. *Eur. J. Inorg. Chem.* **2000**, 2481. (b) Siefert, R.; Weyhermüller, T.; Chaudhuri, P. *J. Chem. Soc., Dalton Trans.* **2000**, 4656. (c) Stinziano-Eveland, R. A.; Nguyen, S. T.; Liable-Sands, L. M.; Rheingold, A. L. *Inorg. Chem.* **2000**, *39*, 2452.

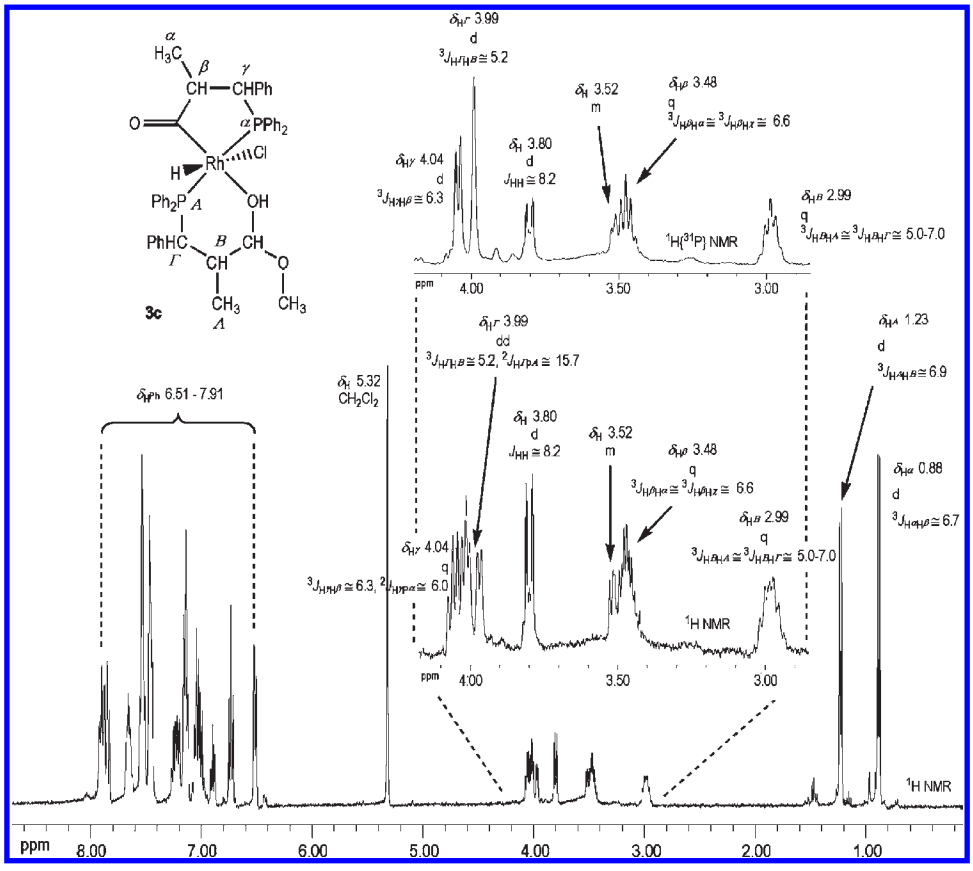

Figure 7. ^{1}H and ^{1}H{^{31}P} NMR spectra ($\delta_H > 0$) of a freshly prepared CD_2Cl_2 solution of diastereomer **3c**.

observed for the in situ MeOH system. The ^{1}H and HMBC ^{1}H/^{13}C{^{1}H} NMR data show that the coordinated hemiacetal component slowly rearranges within an equilibrium to the aldehydic group (Scheme 4): the key data are the generation of a broad singlet at δ_H 9.34, due to a C*H*O proton, and the correlation between the ^{1}H doublet of C*H*$^A_3$CH at δ_H 1.23 and a ^{13}C{^{1}H} singlet at δ_C 215.56 due to an aldehydic C atom. The broadness of −C*H*O possibly implies a coordinated −CHO (requiring a $^{3/2.5}J_{HRh}$ value of ∼2.6) via η^1-O or η^2-C=O (π bond), as illustrated in Scheme 4. Both of the coordination modes are well established for transition metals in general; for Rh, only three aldehyde complexes (all η^1-O) have been structurally characterized,[4a,20] and the C*H*O proton signals are reported as singlets.[4a,20a] The ^{1}H NMR data for the η^2-PC-chelated ligand are unchanged during the establishment of the hemiacetal/aldehyde equilibrium over ∼2 days, when various diastereomers are generated, implying that this phosphine is not involved in the equilibrium processes; in contrast, the ^{1}H NMR signals of the hemiacetal phosphine [i.e., the CHC*H*$_3$ and C*H*-(CH$_3$) protons in the δ_H 0.72−1.54 and δ_H 2.94−4.08 regions, respectively, and the aromatic protons (δ_H ∼ 6.51−7.91)] do vary with time, and this results in the overlapping of such signals for the diastereomers. The ratio of the integrations of, for example, the unchanged C*H*$^{I'}$Ph quintet at δ_H 4.04 (I') and that of the variable C*H*O singlet (I^{Ald}) thus monitors the hemiacetal/aldehyde equilibrium; the I^{Ald}/I' ratio, zero after dissolution of **3c** in CD_2Cl_2, increases to ∼0.36 over 20 h and then decreases to zero after ∼2 days. The sequence of equilibria seen in CD_2Cl_2 among the diastereomers, which shows temporary existence in the aldehyde form, must be brought about by their relative thermodynamic stabilities; their formation must result, at least in part, from a change in the stereochemistry of the hemicacetal/aldehyde C atom (C25).

Studies of the in situ reaction of **P-CHO** with [RhCl(COD)]$_2$ in CD_2Cl_2 at rt (phosphine:Rh = 2) also revealed the rapid formation of diastereomers (labeled **3k** and **3l**; Table S1 in the Supporting Information) in the resulting yellow solution, with an initial **3k**:**3l** ratio of 3.5 slowly increasing and with only **3k** being seen after ∼30 h. The NMR data (Table S1 in the Supporting Information) suggest that **3k** and **3l** are different from the diastereomers formed by dissolution of the isolated **3c** in CD_2Cl_2, implying a role for MeOH and the hemiacetal in the epimerization processes (cf. Scheme 4). A total of nine type **3** hemiacetal diastereomers were detected by NMR in CD_2Cl_2 solutions (Table 1, footnote *c*, and Table S1, footnote *b*, in the Supporting Information) compared to just two seen in CD_3OD (**3a** and **3b**; Table 1, footnote *b*), where no interchange process is apparent or expected.

Iridium Systems. The behavior of the Ir/**P-CHO** systems generally follows that of the Rh systems. Thus, the rt reaction in MeOH of [IrCl(COD)]$_2$ (as a red suspension) with **P-CHO** (phosphine:Ir = 2) results in the immediate dissolution of the Ir precursor and the formation of **4**, an

(20) (a) Carmona, D.; Lamata, M. P.; Viguri, F.; Rodríguez, R.; Oro, L. A.; Balana, A. I.; Lahoz, F. J.; Tejero, T.; Merino, P.; Franco, S.; Montesa, I. *J. Am. Chem. Soc.* **2004**, *126*, 2716. (b) Dias, E. L.; Brookhart, M.; White, P. S. *Chem. Commun.* **2001**, 423.

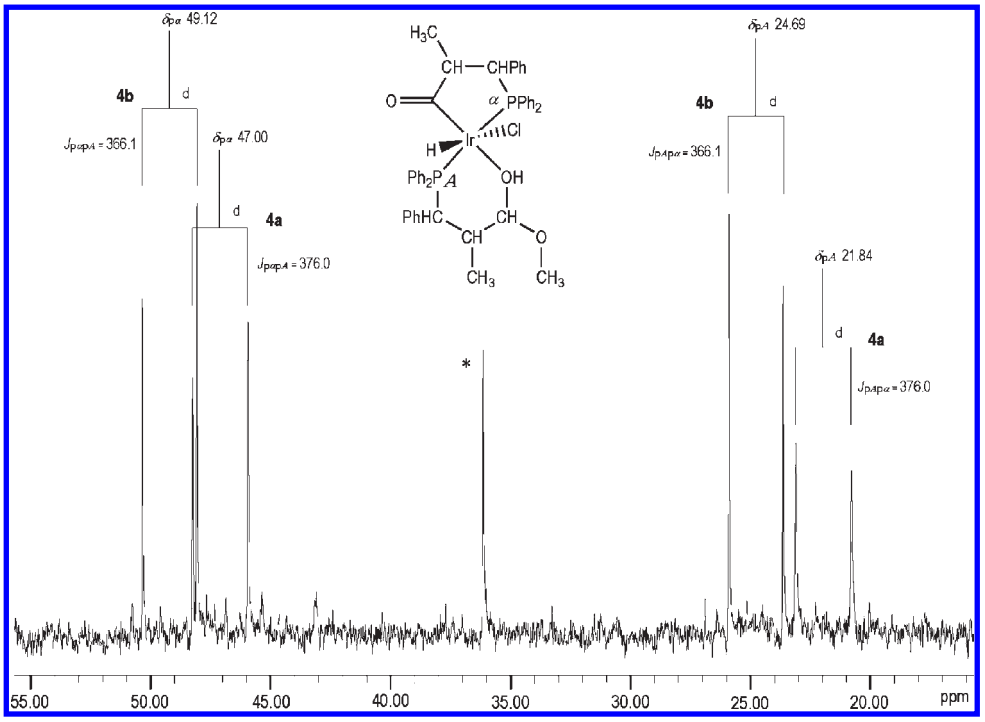

Figure 8. In situ $^{31}P\{^1H\}$ NMR spectrum of a fresh CD_3OD solution of **4**, showing diastereomers **4a** and **4b** (**4a**:**4b** ~ 0.6); * = byproduct (see text).

acylhydrido-chelated hemiacetal phosphine species again with five chiral centers (Scheme 3). The in situ $^{31}P\{^1H\}$ and ^1H NMR spectra "match" those of the in situ Rh system in MeOH, but with no coupling to the metal center: δ_P doublet of doublets are seen immediately for two diastereomers (**4a** and **4b**) in a **4a**:**4b** ratio of ~0.6 (Table 2 and Figure 8), but **4a** precipitates, and after ~1 h, signals are seen only for **4b**. The **4b** resonances are then slowly replaced by those of a third diastereomer (**4c**) in what appears to be an equilibrated solution (Figure S5 in the Supporting Information). [It should be noted that the **a**, **b**, **c**, etc., designations just differentiate isomers of the same compound; the pairs **3a**/**4a**, **3b**/**4b**, **3c**/**4c**, etc., have no particular relationship.] The $^{31}P\{^1H\}$ NMR signals for the diastereomers of type **4** are upfield of those found for type **3** (typical for such Ir^{III} vs Rh^{III} systems[21]), while the large $J_{P\alpha PA}$ coupling constants are again consistent with mutually *trans*-P atoms.[18] The in situ equilibria were also monitored via the high-field ^1H NMR spectra, where pseudotriplets were seen for the hydride ligand of 4a−**4c**, implying that $J_{HP\alpha} \approx J_{HPA}$ (see Table 2).

The precipitated **4a**, an almost colorless, crystalline material, is isolated in ~24% yield, although a satisfactory elemental analysis was not obtained even for a crystal that was shown to be **4**·MeOH; $^{31}P\{^1H\}$ NMR data for isolated **4a** in solution (Figure S6 in the Supporting Information) showed it to contain ~5% of another P-containing compound (see below).

Crystallographic analysis of the X-ray-quality crystals that precipitated as **4a** from the in situ reactions in MeOH revealed that the structure was akin to that of **3c**; one of the two almost identical, independent molecules contained in the asymmetric unit is illustrated in Figure 9.

(21) Marcazzan, P. Ph.D. Dissertation, University of British Columbia, Vancouver, British Columbia, Canada, **2002**; Chapter 3 and references cited therein.

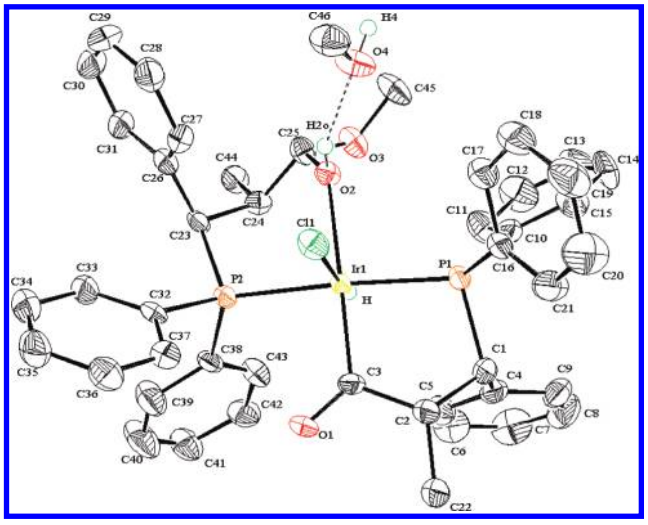

Figure 9. Crystal structure of **4**·MeOH (diastereomer **4a**), with 50% probability ellipsoids.

MeOH is strongly hydrogen-bonded in the same manner as that described for **3c**. There are also four other intermolecular O···H bonds for each of the two independent MeOH solvate molecules; three of these correspond to those described for **3c**, while the fourth one is marginal (O···H = 2.66 Å), between the O4 atom of MeOH and the H atom (H22B) of CH_3 of acylphosphine.

As for **3c**, just two enantiomeric forms of diastereomer **4a** are found in the solid-state structure, and the two independent molecules **4a**-E1 and **4a**-E2 (Figure S2-B in the Supporting Information) show the same stereochemistry as the five C centers of **3c**. The immediate $^{31}P\{^1H\}$ and high-field ^1H NMR spectra of isolated **4a** in a CD_2Cl_2 solution show the presence of essentially only one diastereomer (Table 2 and Figures S6 and S7 in the Supporting Information), and its concentration does not change over 32 h. As for the Rh

analogue, the hydride of **4a** was located by X-ray analysis and IR data in the solid state and in solution, which show also the presence of the acyl carbonyl.

The solid-state structures of **3c** and **4a** (Figures 4 and 9, respectively, and Table 4) are of distorted octahedral geometry, typically associated with Rh^{III} and Ir^{III}, and exhibit similar features. The metal, hydride, chloride, and hydroxyl O atoms and the acyl C atom form an almost perfect plane, while the P1−M−P2 angles of 171−172° reveal the octahedral distortion that results from the chelated phosphines and a small hydride ligand. In both structures, the metal−P1 bond length (of the five-membered ring) is ∼0.06−0.07 Å shorter than the metal−P2 length (of the six-membered ring), and the corresponding metal−P bond lengths are essentially the same; the values are typical of those for alkyl(aryl)phosphine−M (M = Rh, Ir) complexes, as are the M−Cl and M−H bond lengths.[3d,22,23] Within the aroyl group, the C3−O1 and M−C3 bond lengths, as well as the H−M−C3 and O1−C3−M angles (Table 4), are in good agreement with literature values for *cis*-hydrido(*σ*-acyl/aroyl)rhodium[3a,b,d−f,i,k,n] and -iridium complexes.[3c,g,j,n] Such complexes, formed by the oxidative addition of an aldehyde group, are well-known: the first structures of such Rh and Ir complexes were reported in 1991[3k] and 1983,[3p] respectively, and several more Rh[3a,b,d−f,i] and Ir complexes[3c,g,j,n] synthesized in this way have been reported since.

The **3c** and **4a** structures are the first reported for transition-metal complexes with a phosphine ligand chelated via the P atom and a hydroxyl O atom of a hemiacetal group; indeed, there are no reported structures of Rh or Ir complexes with a coordinated hemiacetal. Only nine such structures have been reported for transition metals: three for Ag,[24] one for Mo,[25] and five for lanthanide metals.[26] Structures of Rh complexes with chelated P−O ligands, where the O atom is of an alcohol function, are quite common,[19a,b,27] although we could find no reports on analogous Ir complexes; within **3c**, the Rh−O2 bond length and P−Rh−O2 angles are similar to data for the alcohol-bonded complexes.

Unlike **3**·MeOH, whose formation and solution behavior center on just diastereomers (i.e., the chemistry is free of byproducts), the in situ formation of **4**·MeOH, and a CD_2Cl_2 solution of isolated **4a**, shows the presence of a P-containing byproduct. This is exemplified particularly by in situ reactions of a red solution of $[IrCl(COD)]_2$ in CD_2Cl_2 with **P-CHO**. With **PCHO**:Ir = 2, the resulting yellow solution after ∼40 h contains just **4a**, while in a **PCHO**:Ir = 1 in situ system, the dominant species (>95%) is detected as a singlet at δ_P 50.64. This correlates with a high-field ^{1}H NMR doublet at δ_H −16.51 ($J_{HP} \cong 13.3$), as shown by 2D HSQC $^{31}P\{^1H\}/^1H$ NMR data, and could correspond to the hydridoacyl species Ir(H)Cl(COD)[η^2-*P*,*C*(O)-(Ph_2P)CH(Ph)CH(Me)C(O)] formed by one phosphine coordinated in the η^2-PC mode; however, its isolation has proved impossible. A singlet at δ_P 50.71 was sometimes seen in the in situ CD_3OD system and presumably corresponds to the resonance seen in CD_2Cl_2. Another unidentified byproduct in the Ir system was sometimes seen as a singlet at δ_P ∼35 (Figures S5 and S6 in the Supporting Information), which could represent either a monophosphine complex or a diphosphine complex with equivalent *trans*-P atoms. The presence of these byproducts in isolated **4a** (in contrast to **3c** for the Rh analogue) prevented assignment by 2D methods of all of the ^{1}H and ^{13}C NMR resonances.

The solution behavior of isolated **4**·MeOH in CD_2Cl_2, where only diastereomer **4a** is detected over 32 h (Figure S6 in the Supporting Information), is very different from that shown by such solutions of **3**·MeOH (Figures S3 and S4 in the Supporting Information); consistent with this, there are no changes in the ^{1}H and $^{13}C\{^1H\}$ NMR spectra of **4a** with time, implying that no hemiacetal/aldehyde equilibrium exists in the Ir system. The findings strongly suggest that the detected number of diastereomers for the Rh system, and their varied concentrations, result from such an equilibrium. Whether the byproducts detected in solutions of the Ir system (see previous paragraph) play a role in the solution behavior of the species is unclear. The nature of the solution processes that give rise to the formation of the various diastereomers remains unknown, and it should be noted that in the dissymmetric Rh^{III} and Ir^{III} diastereomers described there is also chirality at the metal center.

A reviewer suggested that in the Rh and Ir systems complexation in solution could be via the OMe group rather than the OH group seen in the solid state, and we have no strong evidence against this possibility; indeed, such bonding could account for some of the detected stereomers. However, we are unaware of such alkoxide bonding from a hemiacetal group and favor OH bonding in solution.

Potential of the Complexes as Precursors for Catalysis. In terms of the potential for homogeneous catalysis, tests should be carried out on solutions containing a single diastereomer that is sufficiently stable in a selected solvent. The findings on the Rh and Ir systems suggest that suitable systems would be a CH_2Cl_2 solution of isolated **3c**, an equilibrated in situ CH_2Cl_2 solution of **3k**, a CH_2Cl_2 solution of isolated **4a**, and an in situ CH_3OH solution containing **4c**. Conversely, an in situ **3** species formed in MeOH is less suitable because of equilibration to other diastereomers. Data on the Pd systems suggest that a CH_2Cl_2 solution of isolated **1** (existing largely as **1a**) might be sufficiently stable to be tested,

(22) Rh systems:(a) Lorenzini, F.; Patrick, B. O.; James, B. R. *Inorg. Chim. Acta* **2008**, *361*, 2123. (b) Sangtrirutnugul, P.; Stradiotto, M.; Tilley, T. D. *Organometallics* **2006**, *25*, 1607. (c) Hartwig, J. F.; Cook, K. S.; Hapke, M.; Incarvito, C. D.; Fan, Y.; Webster, C. E.; Hall, M. B. *J. Am. Chem. Soc.* **2005**, *127*, 2538. (d) Cîrcu, V.; Fernandes, M. A.; Carlton, L. *Polyhedron* **2003**, *22*, 3293. (e) Paneque, M.; Sirol, S.; Trujillo, M.; Gutiérrez-Puebla, E.; Monge, M. A.; Carmona, E. *Angew. Chem., Int. Ed.* **2000**, *39*, 218. (f) Meuting, A. M.; Boyle, P.; Pignolet, L. H. *Inorg. Chem.* **1984**, *23*, 44.

(23) Ir systems:(a) Lorenzini, F.; Marcazzan, P.; Patrick, B. O.; James, B. R. *Can. J. Chem.* **2008**, *86*, 253. (b) Rampf, F. A.; Spiegler, M.; Herrmann, W. A. *J. Organomet. Chem.* **1999**, *582*, 204. (c) Haak, S.; Süss-Fink, G.; Neels, A.; Stœckli-Evans, H. *Polyhedron* **1999**, *18*, 1675.

(24) (a) Koenuma, M.; Kinashi, H.; Ōtake, N.; Sato, S.; Saito, Y. *Acta Crystallogr.* **1976**, *B32*, 1267. (b) Blount, J. F.; Evans, R. H.; Liu, C.-M.; Hermann, T.; Westley, J. W. *Chem. Commun.* **1975**, 853. (c) Blount, J. F.; Westley, J. W. *Chem. Commun.* **1971**, 927.

(25) Liu, S.; Zubieta, J. *Polyhedron* **1989**, *8*, 1213.

(26) (a) Lu, Y.; Deng, G.; Miao, F.; Li, Z. *Carbohydr. Res.* **2004**, *339*, 1689. (b) Yang, L.; Wu, J.; Weng, S.; Jin, X. *J. Mol. Struct.* **2002**, *612*, 49. (c) Yang, L.; Zhao, Y.; Xu, Y.; Jin, X.; Weng, S.; Tian, W.; Wu, J.; Xu, G. *Carbohydr. Res.* **2001**, *334*, 91. (d) Lu, Y.; Guo, J. *Carbohydr. Res.* **2006**, *341*, 683.

(27) For example, see:(a) Duran, J.; Oliver, D.; Polo, A.; Real, J.; Benet-Buchholz, J.; Fontrodona, X. *Tetrahedron: Asymmetry* **2003**, *14*, 2529. (b) Valderrama, M.; Contreras, R.; Araos, G.; Boys, D. *J. Organomet. Chem.* **2001**, *619*, 1. (c) Borns, S.; Kadyrov, R.; Heller, D.; Baumann, W.; Spannenberg, A.; Kempe, R.; Holz, J.; Börner, A. *Eur. J. Inorg. Chem.* **1998**, 1291. (d) Galdecki, Z.; Galdecka, E.; Kowalski, A.; Pruchnik, F. P.; Wajda-Hermanowicz, K.; Starosta, R. *Polym. J. Chem.* **1999**, *73*, 859.

while a CH_2Cl_2 solution of **2** (in situ or isolated) is less attractive. Indeed, the overall findings on the solvent-dependent, hemiacetal/acetal/aldehyde transformations and stereochemical changes within solution species suggest that such chiral phosphinoaldehydes are unlikely to be useful ligands for applications in asymmetric catalysis. Ventures into this area would first require resolution of the racemic **P-CHO** ligand, and this is feasible via its treatment with a chiral alcohol or via the use of a Pd^{II} complex containing an auxiliary chiral ligand; the latter methodology has just been demonstrated by others for a related diphosphine made by the hydrophosphination of a phosphinoaldehyde.[6]

Our studies show that when multiple chiral centers are involved, careful analysis is required to reveal the complexities and limitations when the composition of solution species is being considered for catalysis. Further, the observed oxidative addition of the CHO group in the Rh and Ir systems, with the generaton of octahedral, six-coordinate species, is likely to be unfavorable for a range of catalytic processes, and thus systems that involve a reduction to Rh^I/Ir^I species are likely to be favored.

Conclusions

Described are reactions between Pd^{II}, Rh^I, and Ir^I precursors and our recently synthesized phosphinoaldehyde $(Ph_2P)CH(Ph)CH(Me)CHO$ (labeled **P-CHO**), which was available as a diastereomeric mixture with a dr value of ~20. The Pd^{II} product obtained from a reaction in CH_2Cl_2 is *trans*-$PdCl_2(\eta^1$-*P*-**P-CHO**$)_2$, while in MeOH, the −CHO groups are converted to $-CH(OMe)_2$, the corresponding acetal derivative. The Rh and Ir reactions in CH_2Cl_2 generate products in which one **P-CHO** ligand has undergone oxidative addition to form a *cis*-hydrido(acyl) moiety, while a second **P-CHO** has been converted to the hemiacetal **P-CH(OH)(OMe)**, which is coordinated via the P atom and the hydroxyl O atom; such structural types have not been previously reported. Although there are two chiral C centers in **P-CHO** (and three in the hemiacetal derivative), X-ray structural and NMR data show that isolated complexes exist as just one diastereomer, although in solution other diastereomers can be generated, especially within the Rh system in CD_2Cl_2, where a reversible loss of MeOH from the coordinated, chiral, hemiacetal group sets up a slow equilibrium with a coordinated aldehyde species. Conditions are suggested for testing of the complexes as potential precursor catalysts for catalytic processes, but the systems are likely to be ineffective in asymmetric systems.

Supporting Information Available: Asymmetric units, NMR spectra, and a table of NMR data. This material is available free of charge via the Internet at http://pubs.acs.org.